Survey of the (^{3}He,t) reaction: Excitation of the isobaric analog of the giant dipole resonance

S. L. Tabor
Department of Physics, Florida State University, Tallahassee, Florida 32306
and Department of Physics and Astronomy, University of Maryland, College Park, Maryland 20742

C. C. Chang, M. T. Collins,* G. J. Wagner,† and J. R. Wu‡
Department of Physics and Astronomy, University of Maryland, College Park, Maryland 20742

D. W. Halderson§ and F. Petrovich
Department of Physics, Florida State University, Tallahassee, Florida 32306
(Received 15 January 1981)

The (^{3}He,t) reaction at 130 and 170 MeV has been investigated on targets of ^{12}C, ^{16}O, ^{27}Al, ^{28}Si, ^{40}Ca, ^{46}Ti, and ^{90}Zr. Data for the (^{3}He,^{3}He′) reaction were measured simultaneously for reference purposes. Structure is observed in the spectra from the (^{3}He,^{3}He′) and (^{3}He,t) reactions at the expected positions of the giant quadrupole resonance and the isobaric analog of the giant dipole resonance, respectively. An angular distribution was measured for the suspected giant dipole resonance structure in the ^{40}Ca(^{3}He,t)^{40}Sc reaction at 130 MeV. The data are reasonably described by a collective model calculation based on the Goldhaber-Teller model for the giant dipole resonance. Several other strong peaks at excitation energies below the giant dipole resonance are observed in the (^{3}He,t) spectra. Most notable of these are the ones at the expected positions for analogs of well known 1^+ states and $1\hbar\omega$ stretched states in the targets.

[NUCLEAR REACTIONS ^{12}C, ^{16}O, ^{27}Al, ^{28}Si, ^{46}Ti, ^{90}Zr (^{3}He,t) and (^{3}He,^{3}He′) E=130, 170 MeV; measured $d\sigma/d\Omega$ (E,θ); giant resonances; stretched states.]

I. INTRODUCTION

Perhaps the word "giant" would never have been applied to the dipole resonance if the photon absorption process did not select so strongly the lowest allowed multipole. This selectivity, however, effectively prevents the study of other giant resonances with the technique. Inelastic hadron scattering has proved to be a very useful tool for studying isoscalar multipole resonances, especially the giant quadrupole[1–3] and monopole[4] resonances (GQR and GMR). On the other hand, the inelastic scattering of light ions is not effective in exciting isovector resonances, not even the giant dipole resonance (GDR). The reason is that the isovector term in the effective interaction is sufficiently weak that broad excitations are not visible over the strong continuum background.

One result of this state of affairs is a dichotomy between the two strongest multipole resonances, the GDR and GQR. The GDR has been studied mainly by photonuclear reactions and the time-reversed radiative capture reactions, but is not clearly visible in inelastic hadron scattering. On the other hand, the GQR has been investigated mainly through the inelastic scattering of light nuclei at intermediate energies. In some ways the different selectivity of the two techniques is fortunate because it provides a clean separation of the resonances which are close together in excitation energy and would otherwise overlap as they do in electron scattering. However, the inability to study both resonances with the same experimental approach has generated considerable discussion.

Charge exchange reactions offer the possibility of exciting isovector resonances in a manner similar to inelastic scattering. The problem of stronger isoscalar resonances is eliminated because isoscalar states are completely suppressed in the case of the (^{3}He,t) reaction on T=0 targets. This is because the

final nucleus has $T_Z = -1$ under these conditions and every state has $T \geq 1$. Isoscalar excitations are not forbidden for the (^{3}He,t) reaction on $T \neq 0$ targets, however.

We have used the systematics[2] of the excitation of the GQR by inelastic scattering as a guide in designing the charge exchange experiments. These systematics suggest that intermediate beam energies produce the best GQR peak-to-background ratio and that heavier targets yield narrower peaks with larger fractions of the sum rule strength. For this reason we have used ^{3}He beams of 130 and 170 MeV and have selected the heaviest $T=0$ target, ^{40}Ca, for the most complete study. It is difficult to determine how effective the (^{3}He,t) reaction at lower beam energies is in exciting giant resonances because the published spectra usually do not extend to such high excitation energies. An exception is the survey of Ball and Cerny,[5] where the ^{12}C(^{3}He,t) reaction at 50 MeV does not strongly excite any structure at the GDR energy.

In the ^{40}Ca(^{3}He,t)^{40}Sc reaction at 130 MeV, a broad structure was seen which agrees in energy with the expected position of the analog of the GDR in ^{40}Ca. An angular distribution was measured for this structure as well as for the elastic scattering.

To obtain more information a survey was performed of the (^{3}He,t) reaction at 170 MeV on a variety of targets from ^{12}C to ^{90}Zr. In this case only three angles were measured. A broad peak was seen at the expected GDR energy for all the $T=0$ targets. Structures were also seen on the $T \neq 0$ targets, although the situation is more complicated since isoscalar transitions are possible.

Previous work has led to considerable progress in understanding the analogs of the $M1$ and Gamow-Teller resonances with the (p,n) (Refs. 6–9) and (^{3}He,t) (Refs. 10 and 11) reactions. An example has also been shown of excitation of the GDR in the (n,p) reaction.[12] In the present experiment possible $M1$ states have been seen on several targets. Also seen in the present work are some relatively narrow states which agree systematically in energy with the expected position of the $1\hbar\omega$ stretched states.

II. EXPERIMENTAL PROCEDURE

The following data have been measured (laboratory coordinate system): (1) angular distributions of the ^{40}Ca(^{3}He,t) and ^{40}Ca(^{3}He,^{3}He′) reactions at 130 MeV in 2° steps from 10° through 32°; and (2) spectra from the (^{3}He,t) and (^{3}He,^{3}He′) reactions at 170 MeV and at 10°, 15°, and 20° on targets of ^{12}C, ^{16}O, ^{27}Al, ^{28}Si, ^{40}Ca, ^{46}Ti, and ^{90}Zr.

Beams of 130 and 170 MeV ^{3}He particles from the University of Maryland cyclotron were magnetically analyzed through two 90° bends before reaching the target. The beam optics and collimation were carefully adjusted so that the counting rate on a blank target was insignificant at the most forward angle to be measured.

Target thicknesses were on the order of 1 mg/cm^2. The ^{46}Ti and ^{90}Zr targets were made from isotopically enriched samples, while the other targets had the natural isotopic abundances. Contamination by minority isotopes did not affect the experiment, although a few weak peaks can be seen from them. The self-supporting metallic Ca target was exposed only to an inert atmosphere and otherwise kept under vacuum. The ^{16}O spectrum was obtained by subtracting the spectrum from a Si target from that from a SiO_2 target, normalized by the elastic scattering yields.

For the 130 MeV experiment the tritons were detected and identified with a 1 mm thick Si surface barrier ΔE detector and a 15 mm thick Ortec high-purity Ge E detector. The experiment at 170 MeV used a stack of two 13 mm thick high-purity Ge detectors provided by Pehl and collaborators (Lawrence Berkeley Laboratory) in a cooperative arrangement. Both electrodes on the first Ge wafer were ion implanted to reduce the dead layers and make the detector suitable for the ΔE measurement.

III. RESULTS OF THE 170 MeV SURVEY

The ^{3}He and t spectra measured at a laboratory angle of 15° are shown in Figs. 1–7. The inelastic scattering spectra on top are presented directly as a function of excitation energy in the target nucleus. The charge exchange spectra on the bottom have been shifted by the Coulomb energy differences. For example, the ^{12}N spectrum has been shifted so that its 1^+ ground state (g.s.) lines up with its analog in ^{12}C at 15.11 MeV. The ^{90}Nb spectrum was shifted in the opposite direction so that its 0^+ state at 5.18 MeV lies under its analog, the g.s. of ^{90}Zr. No shift is required for ^{27}Al-^{27}Si or ^{46}Ti-^{46}V because their g.s.'s are isobaric analogs. The insets in these figures are γ-ray total absorption curves[13,14] for the target nuclei. They trace out the classical GDR.

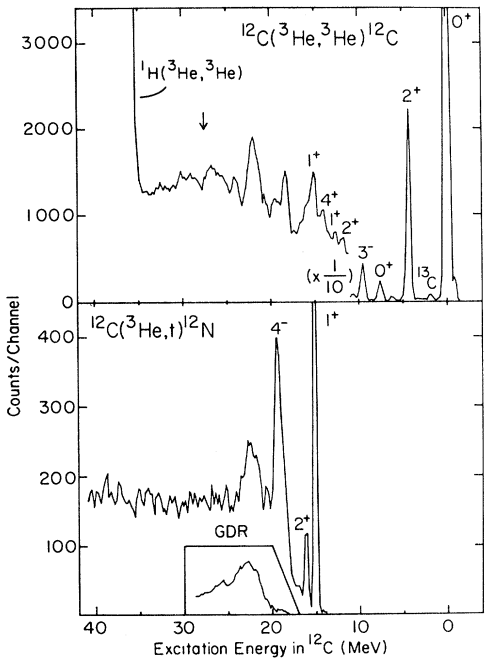

FIG. 1. A comparison of the (^{3}He,^{3}He′) and (^{3}He,t) reactions on ^{12}C at 170 MeV at a laboratory angle of 15°. The ^{12}N spectrum has been shifted by the Coulomb energy difference so that states in ^{12}C and ^{12}N which are isobaric analogs line up. The inset at the bottom labeled "GDR" traces the photoabsorption cross section (Refs. 13 and 14). The arrow in the upper figure indicates $63A^{-1/3}$ MeV.

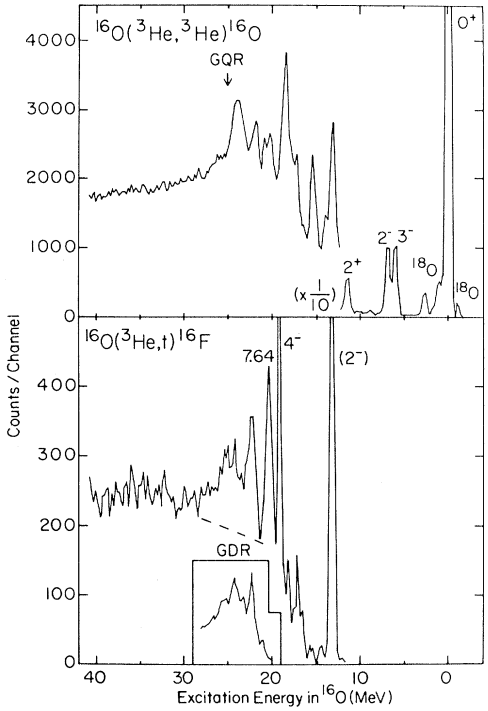

FIG. 2. A comparison of the (^{3}He,^{3}He′) and (^{3}He,t) reactions on ^{16}O at 170 MeV. The arrow labeled "GQR" indicates $63A^{-1/3}$ MeV rather than the centroid of GQR strength in ^{16}O. Refer to the caption of Fig. 1 for more details.

A. Giant quadrupole resonance

Arrows are drawn in the ^{3}He spectra at the excitation energy of $63A^{-1/3}$ MeV. With the exception of ^{12}C, where no definite structure is seen, the arrows are labeled "GQR" for giant quadrupole resonance. Our failure to observe GQR strength in ^{12}C is consistent with earlier work.[15] A plastic material was used for the ^{12}C target, giving rise to a large elastic scattering peak from ^{1}H, whose tail can be seen in Fig. 1.

The association of the observed structures at $E_x \sim 63A^{-1/3}$ MeV with the GQR seems reasonable even though no conservation law excludes the excitation of isovector resonances in ^{3}He scattering. The isovector interaction strength is considerably weaker than the isoscalar strength; consequently, only the isoscalar resonances (GQR, giant monopole resonance, etc.) are expected to be clearly visible in the ^{3}He spectrum. The question of $l=0$ monopole strength (GMR) is still under investigation.[16] Among the targets discussed here monopole strength has been reported[16] only on ^{90}Zr.

The group of peaks to the right of the arrow in ^{16}O has been identified with the GQR in a coincidence decay measurement.[17] The present inelastic ^{3}He scattering spectrum is very similar to that observed[17] in inelastic α scattering, which is basically isoscalar.

With increasing target mass, the detailed structure of the GQR region merges into one broad bump. It is likely that the fine structure spacing simply drops below the widths of the peaks or the experimental energy resolution for larger A. Another trend with increasing mass is that the GQR centroid moves closer to $63A^{-1/3}$ MeV after starting somewhat below that value in ^{16}O.

In general, the position and shape of the GQR structures agree well with previous studies and no further analysis will be presented here.

B. Giant dipole resonance

The systematic appearance over a range of nuclei of a structure which is similar in shape and position

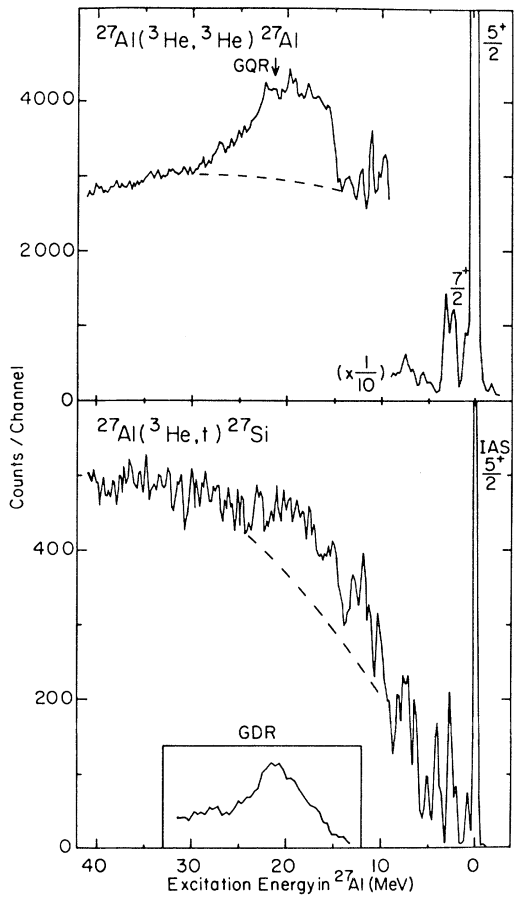

FIG. 3. A comparison of the (^{3}He,^{3}He') and (^{3}He,t) reactions on ^{27}Al at 170 MeV. The dashed lines indicate an estimate of the continuum background. Refer to the caption of Fig. 1 for more details.

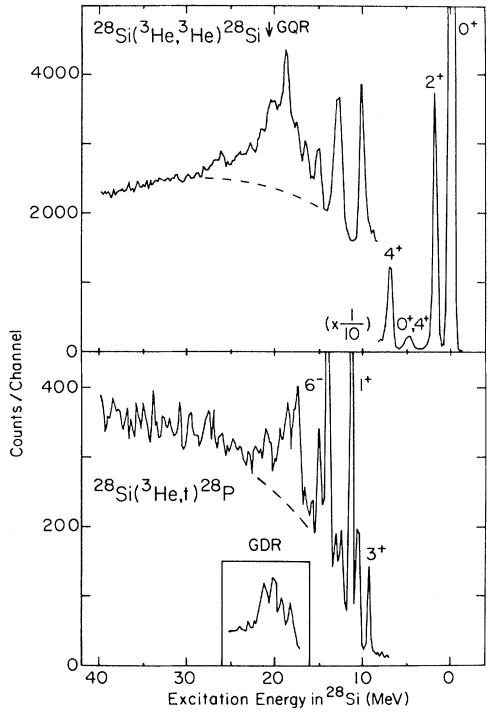

FIG. 4. A comparison of the (^{3}He,^{3}He') and (^{3}He,t) reactions on ^{28}Si at 170 MeV. Refer to the caption of Fig. 1 for more details.

to the GDR as observed in photoabsorption experiments provides important evidence for population of the GDR in the (^{3}He,t) reaction. This can be seen in Figs. 1–7, especially for the $T=0$ targets. The comparison is made between the photoabsorption spectrum on the target nucleus and the spectrum of the final nucleus shifted by the Coulomb energy difference. That is, the structure seen in the final nucleus appears to be the isobaric analog of the GDR built on the g.s. of the target nucleus.

The charge exchange-photoabsorption comparison is good for ^{12}C and excellent for ^{16}O, where some details of the structure are reproduced. In ^{28}Si the broad bumps of the GDR agree, but the detailed structure does not. Perhaps this is related to its position near the middle of the *s-d* shell. The agreement is better in ^{40}Ca.

The situation is more complicated in $T\neq 0$ nuclei, where more than one isospin component of the GDR can be excited and the agreement in the spectra is not as good. A bump probably corresponding to multiple isospin components of the GDR is seen on the ^{27}Al, ^{46}Ti, and ^{90}Zr targets. The structure in ^{90}Zr has been assigned $E1$ by other workers.[8,9] The ^{27}Al(^{3}He,t)^{27}Si spectrum (which may contain $T=\frac{1}{2}$ and $T=\frac{3}{2}$ components of the GDR) may be compared with an ^{27}Al(n,p)^{27}Mg spectrum[12] (which contains only the $T=\frac{3}{2}$ component). Although the comparison is limited by background uncertainties and counting statistics, the GDR peak in the former spectrum may be somewhat broader on the low excitation energy side.

The question of the behavior of the continuum background in the t spectra affects the comparison with the photoabsorption spectra. This is especially true of the high-excitation tails of the GDR, which may or may not be in the t spectra, depending on the choice of background. Some background estimates are drawn as dashed lines in the figures. Another factor in the comparison between the GDR and its isobaric analog in the neighboring nucleus is the effect of Thomas-Ehrman shifts.[18] They could

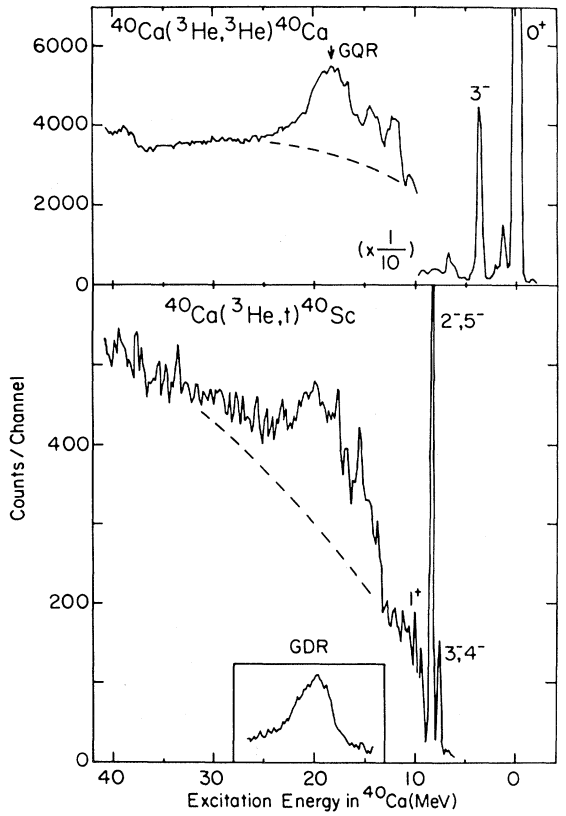

FIG. 5. A comparison of the (^{3}He,^{3}He′) and (^{3}He,t) reactions on ^{40}Ca at 170 MeV. Refer to the caption of Fig. 1 for more details.

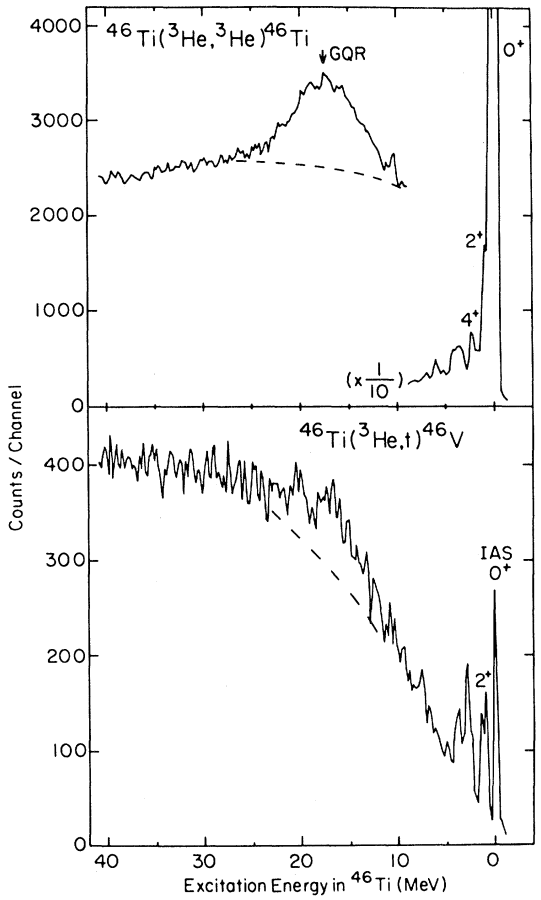

FIG. 6. A comparison of the (^{3}He,^{3}He′) and (^{3}He,t) reactions on ^{46}Ti at 170 MeV. Refer to the caption of Fig. 1 for more details.

result in either an overall shift of the bump or a change in its fine structure, if different GDR components shift differently.

Since this experiment was planned as a target survey, only a few angles were measured for each target. Those fragmentary angular distributions are shown in Fig. 8 to give the reader an idea of the size of the cross sections. A more complete angular distribution will be discussed below. The yields are fairly similar at 15°, clustering around 500 μb/sr. The uncertainties in the cross section values are on the order of $\pm$30%, owing to the difficulty in determining the background.

C. $M1$ strength

The region of $M1$ strength in ^{90}Nb which is labeled "GT" (Gamow-Teller) has been studied extensively in the (p,n) (Refs. 6–9) and (^{3}He,t) (Refs. 10 and 11) reactions. Other 1^+ states are also strongly populated in the charge exchange reaction. These include the g.s. of ^{12}N and probably the 2.08 MeV level[19] in ^{28}P.

The small peak labeled "1^+" in the 15° ^{40}Sc spectrum of Fig. 5 becomes the tallest peak at more forward angles. The spectra of Fig. 9 have been summed over several angles to improve the statistical accuracy. The 1^+ state of ^{40}Sc, which is labeled "3" in the 170 MeV spectrum of Fig. 9, stands out mainly because of the inclusion of the 10° point. The 1^+ peak is also strong at 130 MeV in the forward angle spectra which were not included in the spectrum of Fig. 9. The state lies at an energy of 2.37 MeV in ^{40}Sc and appears to be the analog of a 1^+ state in ^{40}Ca at 10.32 MeV which has been observed as a strong $M1$ transition in inelastic electron scattering.[20] A comparison of the Coulomb corrected energies is given in Table I and discussed further in Sec. III D.

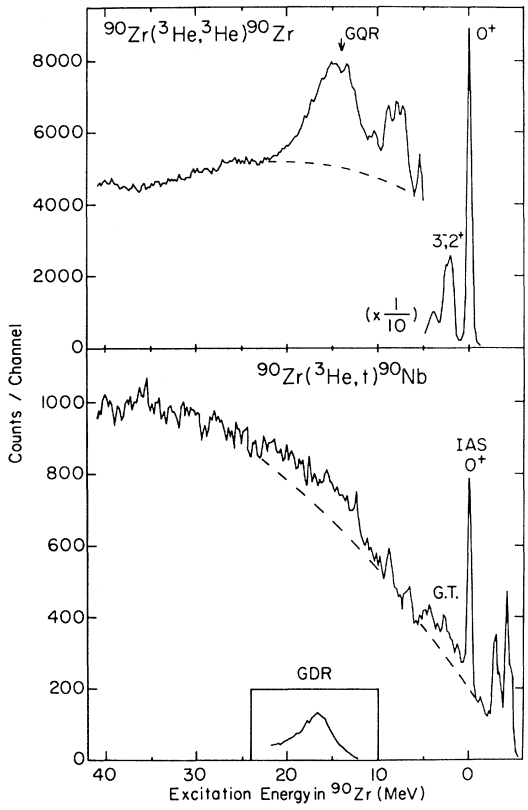

FIG. 7. A comparison of the (^{3}He,^{3}He′) and (^{3}He,t) reactions on ^{90}Zr at 170 MeV. Refer to the caption of Fig. 1 for more details.

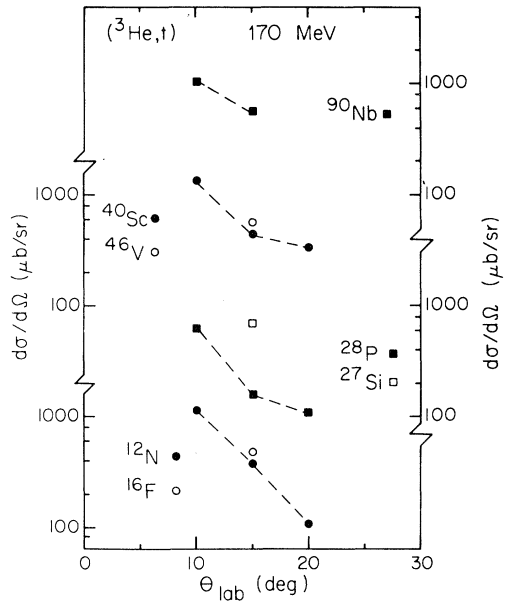

FIG. 8. Angular distributions for the (^{3}He,t) reaction to the GDR in the indicated final nuclides. Data points marked by circles refer to the cross section scales on the left and those marked by squares refer to the scales on the right.

D. Stretched states

The $1\hbar\omega$ strentched states have attracted considerable interest because of their selective population in some intermediate energy reactions and their relatively simple structure. They are characterized by having the highest spin possible for a 1p-1h state formed by promoting the particle up one major shell. The dominant configuration for these states is $(d_{5/2}P_{3/2}^{-1})4^-$ or $(f_{7/2}d_{5/2}^{-1})6^-$, etc., depending on which orbitals are filled. They have been seen in back-angle electron scattering[21–28] and in proton[27,29,30] and pion[31,32] inelastic scattering.

Strong lines are seen in the ^{12}N, ^{16}F, and ^{28}P spectra which appear to be the analogs of known high-spin $T=1$ stretched states in ^{12}C,[21,22] ^{16}O,[23,24,29,31] and ^{28}Si.[25,26,30,32–34] These tentative assignments are based on the similarity of excitation energies between the known states and their analogs and on their systematic appearance for all the $T=0$ targets where stretched states have been identified. The excitation energies of the analog stretched states are

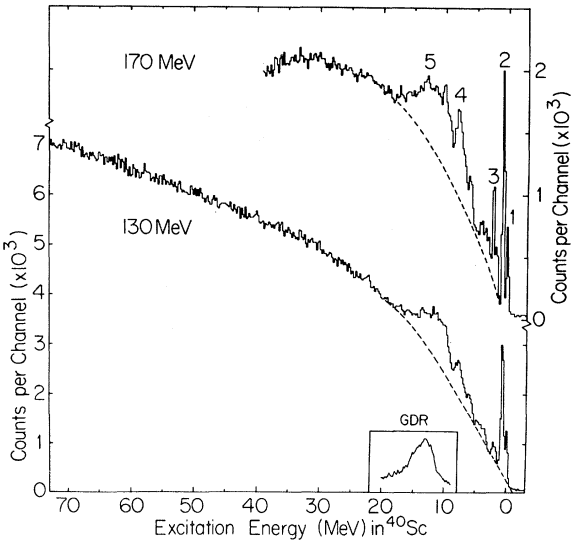

FIG. 9. ^{40}Ca(^{3}He,t)^{40}Sc spectra at the indicated laboratory beam energies. After conversion to excitation energy, the spectra have been summed over the following laboratory angles of observation: at 130 MeV, 20°, 22°, 24°, 26°, 28°, 30°, and 32°; at 170 MeV, 10°, 15°, and 20°. The dashed lines represent estimates of the continuum background as discussed in the text. The inset is adapted from Ref. 13.

TABLE I. A comparison of $T=1$ level energies for isobaric multiplets.

Nucleus	Breakup energy (MeV)	Excitation energy (MeV)	Coulomb corrected (MeV)	Analog State Nucleus	Analog State Energy (MeV)	J^π
^{12}N	0.601	4.28	19.39	^{12}C	19.6[a]	4^-
^{16}F	−0.548	6.40	19.20	^{16}O	18.98[b]	4^-
^{28}P	2.064	2.08	11.40	^{28}Si	11.445[c]	1^+
		4.74	14.06		14.356[d]	6^-
^{28}Al	7.73	5.165[e]	14.481	^{28}Si	14.356[d]	6^-
^{40}Sc	0.534	2.37	10.03	^{40}Ca	10.320[f]	1^+

[a]References 21 and 22.
[b]References 23, 24, 29, and 31.
[c]Reference 19.
[d]References 25, 26, 30, 32, and 33.
[e]Reference 35.
[f]Reference 20.

compared in Table I. Also included in this table are some 1^+ states and the known 6^- state in ^{28}Al. The Coulomb corrected energies in the $T=1$ nuclei are obtained by adding the excitation energy of the lowest $T=1$ state in the $T_Z=0$ nucleus to the observed excitation energy in the $T_Z=\pm 1$ nucleus. The breakup energy is the threshold energy for particle emission.

Table I shows that the Coulomb corrected energies in the $T_Z=-1$ nuclei are generally a few hundred keV lower than in the $T_Z=0$ analogs. Differences of this magnitude in Coulomb energies can be expected between states of different spin and between bound and unbound states (Thomas-Ehrman shift[18]). The Coulomb corrections were determined from the g.s.'s which are usually bound (see Table I), while the stretched states are unbound to proton decay. The only $T_Z=-1$ nucleus with a higher corrected energy for the stretched state is ^{16}F, whose g.s. is also unbound. Another factor in this case is the observation[31] of isospin mixing in the 4^- levels of ^{16}O. The 6^- state[35] in ^{28}Al ($T_Z=+1$) has a higher Coulomb corrected energy than its analog in ^{28}Si, in agreement with these systematics.

The possible 1^+ state in ^{28}P at 2.08 MeV is much closer in corrected energy to its analog, but it is effectively bound to particle decay. Evidence has been shown[26] for 2^+ or 4^+ strength in ^{28}Si at about this energy, so the 1^+ assignment remains tentative until a complete angular distribution can be measured. There is also a 6^- $T=0$ state at a similar energy in ^{28}Si which has been seen in proton[30] and pion[32] scattering, but that state cannot have an analog in ^{28}P.

IV. RESULTS OF THE ANGULAR DISTRIBUTION AND CALCULATION AT 130 MeV

Spectra from the ^{40}Ca(^{3}He,t)^{40}Sc reaction at 130 and 170 MeV have been summed over several angles of observation for presentation in Fig. 9. They are graphed as a function of excitation energy in ^{40}Sc, rather than excitation in the target nucleus as in Figs. 1–7. The inset shows the γ-ray total absorption curve[13] for ^{40}Ca shifted by the Coulomb energy difference of 7.659 MeV to correspond to the excitation energy scale in ^{40}Sc. The peak labeled "1" contains the 4^- ground state and 3^- first excited state at 34 keV in ^{40}Sc. Peak 2 contains the 2^-,5^- doublet at 772 and 892 keV. Peak 3 appears to be a 1^+ state (Sec. III C) and peak 4 has not been satisfactorily identified yet. Peak 5 has the expected energy of the GDR.

An angular distribution of the elastic scattering cross section relative to Rutherford is shown in Fig. 10 along with an optical model fit using code JIB.[36] Real and imaginary potentials of volume Woods-Saxon shape were used with the following parameters: $V=87.73$ MeV, $r_0=1.292$ fm, $a=0.815$ fm, $w=18.36$ MeV, $r_0'=1.651$ fm, and $a'=0.556$ fm.

An angular distribution is presented in Fig. 11 for the GDR peak in the ^{40}Ca(^{3}He,t)^{40}Sc reaction at 130 MeV. The shape of the continuum background under the broad giant resonance peaks is a source of some uncertainty in inelastic hadron scattering, and the (^{3}He,t) reaction is no better. To determine the GDR yields for the angular distribution, a quadratic background shape was fitted at each angle to regions above and below the GDR peak.

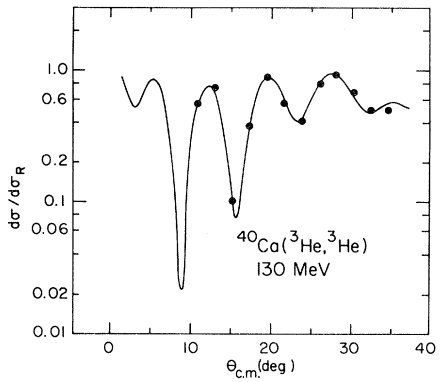

FIG. 10. Angular distribution for the elastic scattering of ^{3}He on ^{40}Ca at a laboratory energy of 130 MeV. The smooth curve is an optical model fit to the data, as discussed in the text.

In the Goldhaber-Teller model of the GDR, the excitation is described by rigid neutron and proton spheres vibrating against each other. With some simplifying assumptions, the transition operator for excitation of the GDR takes the form

$$\Delta 0(\vec{r}_p)=\left[\frac{4\pi}{3}\right]^{1/2}\frac{2NZ}{A^2}\frac{dU_1(r_p)}{dr_p}\vec{d}\cdot\vec{Y}_1(\hat{r}_p)\ ,$$

where $U_1(r_p)$ is the symmetry potential. The essential part of the matrix element of this operator taken between the g.s. and the GDR gives the form factor

$$F(\vec{r}_p)=\sqrt{2}\left[\frac{4\pi}{3}\right]^{1/2}\frac{2}{A}\left[\frac{ZN}{A}\right]^{1/2}\frac{dU_1(r_p)}{dr_p}\times\left[\frac{\hbar^2}{2mE}\right]^{1/2}Y^*_{lm}(\hat{r}_p)\ .$$

Conventional DWBA codes include form factors of the form

$$\frac{\beta_L}{\sqrt{2L+1}}R\frac{dU(r_p)}{dr_p}Y_L(\hat{r}_p)\ ,$$

which can be used for this calculation provided

$$\beta_1=\frac{2}{A}\left[4\pi\frac{ZN}{A}\frac{\hbar^2}{2mE}\right]^{1/2}\ ,$$

and the values of U_1/R are entered for the potential strengths. For the charge exchange reaction there is an additional factor of $\sqrt{2}$ to account for the isospin dependence of the projectile.

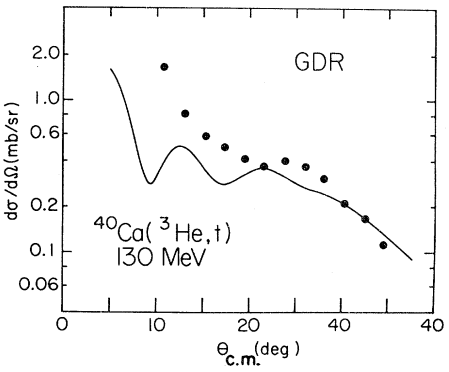

FIG. 11. Angular distribution for the GDR excited by the ^{40}Ca(^{3}He,t)^{40}Sc reaction at 130 MeV. The smooth curve represents the DWBA calculation discussed in the text.

A knowledge of $U_1(r)$ for ^{3}He is needed. As an approximation we will assume that $U_1(r)$ is related to the ^{3}He elastic scattering potential in the same manner as the nucleon symmetry potential is related to the elastic scattering potential as derived from global fits[37–39] to nucleon scattering evaluated for 43 MeV protons. These considerations suggest that the symmetry potential should contain a real volume term and a surface imaginary term. The real term should have the same geometry as the isoscalar volume potential and 0.55 times the strength. The surface imaginary term should have a strength roughly 1.5 times greater and a radius 0.36 fm smaller than the isoscalar imaginary term, which is a combination of volume and surface shapes. These values are based on the best-fit potential for ^{40}Ca which shows[37–39] an anomously large imaginary radius relative to the global parameters. An additional reduction by a factor of 3 is required because only one nucleon in the projectile participates in the charge exchange.

Altogether these considerations suggest using an effective β_1 value of 0.27, a real symmetry potential with parameters $V_1=10.92$ MeV, $r_0=1.292$ fm, and $a=0.815$ fm, and an imaginary surface term with $W_{D1}=6.23$ MeV, $r_0'=1.29$ MeV, and $a'=0.556$ fm.

The results of this calculation are shown in Fig. 11 along with the data. The results are consistent with the assumption that the peak is predominantly the analog of the GDR, although contributions from other multipolarities cannot be ruled out. A slight increase in the radius of the imaginary surface term which is the least well determined parameter would correct the discrepancy in magnitude.

V. CONCLUSIONS

The (^{3}He,t) charge exchange reaction at 130 and 170 MeV appears to systematically excite the iso-

vector GDR and thus provides a complement to the inelastic ^{3}He scattering reaction which preferentially excites the isoscalar resonances. Together these two reactions provide a means of populating the strongest giant multipole resonances in a more similar, but isospin selective, way. Hence, the ^{3}He induced reactions provide a "T meter" for giant resonance studies.

Evidence for population of the GDR comes from a comparison of the Coulomb-shifted (^{3}He,t) spectra with the GDR photoabsorption curves. The two curves are generally similar for $T=0$ targets, suggesting that the structures in the triton spectra are the analogs of the GDR built on the g.s.'s of the targets. The agreement between the curves is not as good for the $T\neq 0$ targets, where the (^{3}He,t) reaction can also excite the antianalog of the GDR. The calculated GDR angular distribution agrees in magnitude and approximate shape with the measured one at 130 MeV for ^{40}Ca.

Intermediate energy charge-exchange reactions are also effective in exciting magnetic transitions, especially $M1$ and Gamow-Teller transitions. Strong $M1$ transitions were seen with the (^{3}He,t) reaction on the ^{12}C, ^{40}Ca, and possibly ^{28}Si targets.

The apparent systematic excitation of isovector $1\hbar\omega$ stretched states is particularly striking in the triton spectra. The (^{3}He,t) reaction offers a new approach to the study of such states. Since the charge exchange reaction populates the analogs of the states in the stable target nuclei, it provides information not obtainable from inelastic scattering.

ACKNOWLEDGMENTS

We are pleased to acknowledge informative discussions with R. A. Lindgren and D. Robson. This work was supported in part by the National Science Foundation.

---

*Present address: Physics Division, Brookhaven National Laboratory, Upton, New York 11973.

†Permanent address: Max-Planck-Institut für Kernphysik, 6900 Heidelberg, West Germany.

‡Present address: Bell Laboratories, Naperville, Illinois 60540.

§Present address: Physics Department, Western Michigan University, Kalamazoo, Michigan 49001.

[1]G. R. Satchler, Nucl. Phys. A195, 1 (1972).

[2]F. E. Bertrand, Annu. Rev. Nucl. Sci. 26, 457 (1976).

[3]G. J. Wagner, in *Giant Multipole Resonances,* edited by F. E. Bertrand (Harwood-Academic, New York, 1980), p. 251.

[4]D. H. Youngblood, C. M. Rozsa, J. M. Moss, D. R. Brown, and J. D. Bronson, Phys. Rev. Lett. 39, 1188 (1977).

[5]G. C. Ball and J. Cerny, Phys. Rev. 177, 1466 (1969).

[6]R. R. Doering, A. Galonsky, D. M. Patterson, and G. F. Bertsch, Phys. Rev. Lett. 35, 1691 (1975).

[7]C. D. Goodman, C. A. Goulding, M. B. Greenfield, J. Rapaport, D. E. Bainum, C. C. Foster, W. G. Love, and F. Petrovich, Phys. Rev. Lett. 44, 1755 (1980).

[8]D. E. Bainum, J. Rapaport, C. D. Goodman, D. J. Horen, C. C. Foster, M. B. Greenfield, and C. A. Goulding, Phys. Rev. Lett. 44, 1751 (1980).

[9]W. A. Sterrenburg, S. M. Austin, R. P. DeVito, and A. Galonsky, Phys. Rev. Lett. 45, 1839 (1980).

[10]A. Galonsky, J. P. Didelez, A. Djaloeis, and W. Oelert, Phys. Lett. 74B, 176 (1978).

[11]D. Ovazza, A. Willis, M. Morlet, N. Marty, P. Martin, P. deSaintinon, and M. Buenerd, Phys. Rev. C 18, 2438 (1978).

[12]F. P. Brady, N. S. P. King, M. W. McNaughton, and G. R. Satchler, Phys. Rev. Lett. 36, 15 (1976).

[13]J. Ahrens, H. Borchert, K. H. Czock, H. B. Eppler, H. Gimm, H. Gundrum, M. Kröning, P. Riehn, G. Sita Ram, A. Zieger, and B. Ziegler, Nucl. Phys. A251, 479 (1975).

[14]B. L. Berman and S. C. Fultz, Rev. Mod. Phys. 47, 713 (1975).

[15]H. Riedesel, K. T. Knöpfle, H. Breuer, P. Doll, G. Mairle, and G. J. Wagner, Phys. Rev. Lett. 41, 377 (1978).

[16]D. H. Youngblood, in *Giant Multipole Resonances,* edited by F. E. Bertrand (Harwood-Academic, New York, 1980), p. 113.

[17]K. T. Knöpfle, G. J. Wagner, P. Paul, H. Breuer, C. Mayer-Böricke, M. Rogge, and P. Turek, Phys. Lett. 74B, 191 (1978).

[18]J. A. Nolen, Jr. and J. P. Schiffer, Annu. Rev. Nucl. Sci. 19, 471 (1969).

[19]R. Schneider, A. Richter, A. Schwierczinski, E. Spamer, and O. Titze, Nucl. Phys. A323, 13 (1979).

[20]W. Gross, D. Meyer, A. Richter, E. Spamer, O. Titze, and W. Knüpfer, Phys. Lett. 84B, 296 (1979).

[21]T. W. Donnelly, J. D. Walecka, I. Sick, and E. B. Hughes, Phys. Rev. Lett. 21, 1196 (1968).

[22]L. W. Fagg, P. B. Ertel, H. Crannell, R. A. Lindgren, J. B. Flanz, and G. B. Peterson, Bull. Am. Phys. Soc. 23, 583 (1978).

[23]I. Sick, E. B. Hughes, T. W. Donnelly, J. D. Walecka, and G. E. Walker, Phys. Rev. Lett: 23, 1117 (1969).

[24]C. Hyde, W. Bertozzi, T. Buti, M. Deady, W. Herman, S. Kelly, S. Kowalski, R. Lourie, B. Pugh, C. P. Sargent, W. Turchinetz, B. Norum, B. L. Berman, M. V. Hynes, J. Lichtenstadt, F. Petrovich, D. Halderson, J. Korr, and W. G. Love, Bull. Am. Phys. Soc. 26, 27 (1981).

[25]S. Yen, R. Sobie, H. Zarek, B. O. Pich, T. E. Drake, C. F. Williamson, S. Kowalski, and C. P. Sargent, Phys. Lett. 93B, 250 (1980).

[26]T. W. Donnelly, J. D. Walecka, G. E. Walker, and I. Sick, Phys. Lett. 32B, 545 (1970).

[27]R. A. Lindgren, W. J. Gerace, A. D. Bacher, W. G. Love, and F. Petrovich, Phys. Rev. Lett. 42, 1524 (1979).

[28]R. A. Lindgren, C. F. Williamson, and S. Kowalski, Phys. Rev. Lett. 40, 504 (1978).

[29]R. S. Henderson *et al.*, Aust. J. Phys. 32, 411 (1979).

[30]G. S. Adams, A. D. Bacher, G. T. Emery, W. P. Jones, R. T. Kouzes, D. W. Miller, A. Picklesimer, and G. E. Walker, Phys. Rev. Lett. 38, 1387 (1977).

[31]D. B. Holtkamp, W. J. Braithwaite, W. Cottingame, S. J. Greene, R. J. Joseph, C. Fred Moore, C. L. Morris, J. Piffaretti, E. R. Siciliano, H. A. Thiessen, and D. Dehnhard, Phys. Rev. Lett. 45, 420 (1980).

[32]C. Olmer, B. Zeidman, D. F. Geesaman, T. S. H. Lee, R. E. Segel, L. W. Swenson, R. C. Boudrie, G. S Blanpied, H. A. Thiessen, C. L. Morris, and R. E. Anderson, Phys. Rev. Lett. 43, 612 (1979).

[33]G. F. Neal and S. T. Lam, Phys. Lett. 45B, 127 (1973).

[34]Dean Halderson, K. W. Kemper, J. D. Fox, R. O. Nelson, E. G. Bilpuch, C. R. Westerfeldt, and G. E. Mitchell, Phys. Rev. C 24, 786 (1981).

[35]R. M. Freeman, F. Haas, A. R. Achari, and R. Modjtahed-Zadeh, Phys. Rev. C 11, 1948 (1975).

[36]F. G. Perey, Oak Ridge National Laboratory Report ORNL-3429, 1973; modified by A. Obst.

[37]F. D. Bechetti, Jr. and G. W. Greenlees, Phys. Rev. 182, 1190 (1969).

[38]M. P. Fricke, E. E. Gross, B. J. Morton, and A. Zucker, Phys. Rev. 156, 1207 (1967).

[39]C. B. Fulmer, J. B. Ball, A. Scott, and M. L. Whiten, Phys. Rev. 181, 1565 (1969).